

**Pressure Dependence of the Magnetic Response of the $S = 1$ Polymeric Chain
[Ni(HF₂)(3-Clpy)₄]BF₄**

Jaynise M. Pérez^{†‡}, Marcus Prepah[†], Pedro A. Quientero[†], Jamie L. Manson[‡],
and Mark W. Meisel[†]

[†] Department of Physics and the National High Magnetic Field Laboratory,
University of Florida, Gainesville, Florida 32611-8440

[‡] Department of Chemistry and Biochemistry, Eastern Washington University,
Cheney, Washington 99004

[‡] Permanent address: Physics, University of Puerto Rico at Mayagüez, Puerto Rico 00681-9000

End of Project Report for the Summer 2015 UF Physics REU Program
sponsored by the National Science Foundation (NSF) via DMR-1461019

Date: July 28, 2015 [some edits (grant numbers and references) by MWM prior to web-posting]

Abstract

[Ni(HF₂)(3-Clpy)₄]BF₄ (py=pyridine) is an $S = 1$ antiferromagnetic polymeric chain with a single-ion anisotropy of $D = 4.3$ K on zero-field splitting and intrachain exchange interaction value of $J = 4.86$ K as previously found at ambient pressure. The ratio of these parameters ($D/J = 0.88$) places this system close to a quantum critical point QCP, where $D/J \approx 1$ falls between the Haldane and the Large-D phase. The temperature dependence of the low-field (100 G and 1 kG) magnetic susceptibility was studied measured as a function of pressure applied by a homemade piston-clamp cell. The temperature decreased with different pressure values in a field of $B = 1$ kG. The high pressure measurement, $P \approx 1.5$ GPa, indicated a significant reduction of the pressure dependency by reducing to a high degree the J value along with the paramagnetic contribution factor.

1. Introduction

To date, the quantum critical point (QCP) between the Haldane and Large-D phases of $S = 1$ spin chains has only been explored theoretically [1]. The Hamiltonian for an one-dimensional, $S = 1$ model in a magnetic field can be written as

$$H = J \sum_i \{ (S_i^x S_{i+1}^x + S_i^y S_{i+1}^y + \beta S_i^z S_{i+1}^z) - D(S_i^z)^2 + E[(S_i^x)^2 - (S_i^y)^2] \} - \vec{B} \cdot \vec{g} \cdot \vec{S} \quad (1.1)$$

where i , indicates that the summation is over the nearest-neighbor spins i and $i + 1$, J stands for the nearest-neighbor intrachain magnetic exchange and the parameters D and E denotes the single-ion anisotropy and rhombic anisotropy, respectively [1]. It has been previously recognized that the one dimensional polymeric chain $[\text{Ni}(\text{HF}_2)(3\text{-Clpy})_4]\text{BF}_4$ (Figure 1) exhibits an exchange anisotropy $J = 4.86$ K, along with a single-ion anisotropy of $D = 4.3$ K at ambient pressure. The ratio of these ($D/J = 0.88$) places this system close to the QCP, when $D/J \approx 1$ from the Haldane state to the Large-D phase. For the purpose of trying to tune the material towards or away from the QCP, the objective of this study is to explore and analyze the magnetic response of the material under pressure using a magnetometer at low temperatures, down to 2 K

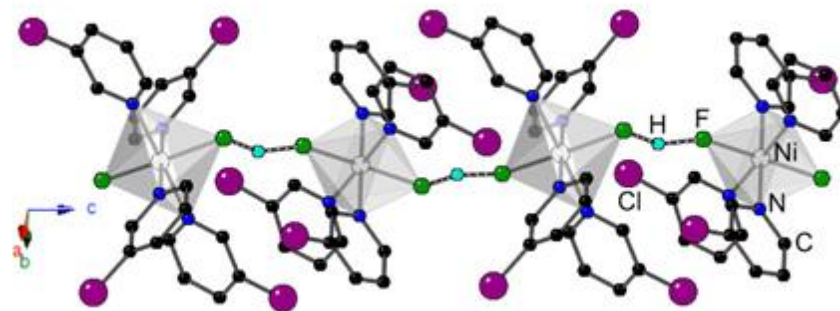


Figure 1. Crystal Structure segment of $[\text{Ni}(\text{HF}_2)(3\text{-Clpy})_4]\text{BF}_4$ (py = pyridine) Ni^{2+} ions linked by F-H-F bridges along the c-axis. Molar mass: 638.68 g/mol. Acquired from: Manson, Jamie L. et al [2].

The measurements were performed in two stages. Specifically, the first measurement was made in a standard sample-holder for the purpose of confirming that the magnetic response of the material was not compromised by the oil needed in the pressure study. Zero field cooling (ZFC) and field cooling (FC) processes were performed as protocols in the sequence file to obtain the measurement. Secondly, the experiments were conducted with a small amount of the initial sample

and oil transferred to the homemade piston-clamp pressure cell. A piece of lead (Pb) was placed into the holder of the pressure cell and used as a manometer in order to measure the pressure. A superconducting quantum interference device (SQUID) magnetometer was used as the instrument for measuring the magnetic moment of the sample at low temperatures.

The magnetometer performs a measurement of the magnetic moment (M /emu*G) vs. Temperature (T /K). The relation used in order to obtain the signature curve of the exchange interaction comes from the susceptibility, defined as

$$\chi = M/H \quad (1.2)$$

where M is the magnetic moment and H is the applied magnetic field. Lastly, taking the data of the susceptibility as a function of the temperature, the exchange interaction value was acquired. This was made by adjusting the parameters of g and J from the Padé approximation and the Curie temperature in order to find the possible paramagnetic (PM) and antiferromagnetic (AFM) components $\chi = \chi_p + \chi_A$ that contributes to the actual data [3].

The results of our first measurement matched the “finger print” from J.L. Manson [2] data at low temperatures. Furthermore, just one measurement with a fairly distinct pressure was achieved. Only the high pressure measurement (~1.49 GPa.) shows a noticeable distinct behavior as compared to the ambient and close to ambient pressure measurements. On the high pressure data it is shown that the AFM component suppresses the PM component. This effect supports the fact that the J value as well as the PM factor both appear to decrease with increasing pressure. This last conclusion needs further investigation since it is being relied on one distinct pressure measurement. From comparison, it can be shown that the intrachain exchange interaction value (J) decreased a 63% from ambient to $P \approx 1.49 \text{ GPa}$.

2. Experiment Details and Data Analysis

2.1 First study: Preliminary Characterization of sample in presence of oil

Using a 7 T SQUID (superconducting quantum interference device) magnetometer equipped with a magnetic property measurement system (MPMS) transport rod (see Appendix), magnetization measurements were performed as a function of temperature to obtain $M(T)$ for

$[\text{Ni}(\text{HF}_2)(3\text{-Clpy})_4]\text{BF}_4$, which came from a sample batch provided by coauthor Jamie L. Manson during his visit to UF on 19 March 2015. The sample vial was labelled “JLM 02-051: $\text{Ni}(\text{BF}_4)_2 + \text{NH}_4\text{HF}_2 + 3\text{-Clpy}$ ”. This first study without externally applied pressure was made in order to characterize the magnetic response of the sample in the presence of the oil needed for the pressure experiments. Initially, a measurement of the sample holder, a low density polyethylene (LDPE) can along with Daphne oil was used in order to subtract the background signal from the forthcoming sample measurement. Afterwards, the sample was inserted into the can along with the Daphne oil (Appendix A), which acts as a pressure transmitting medium for future pressure application. At low temperatures, $T \approx 2 \text{ K}$, the minimal relaxation ($\approx 0.2 \text{ GPa}$) of this oil makes it optimal for the pressure performances [4].

The prepared sample is then placed in a clear drinking straw using a paper lantern cut to secure the can in place and lastly mounted into the transport road. This preliminary measurement, besides providing information about the magnetic functionality of the sample, leads to the analysis on whether or not the oil interacts with the sample in a way that could alter its magnetic properties. Zero field cooling (ZFC) and field cooling (FC) conditions were used as protocols for the measurements in the sequence. In the initial part of the sequence, the sample temperature was lowered to $T=2 \text{ K}$ without applying a magnetic field, this is known as the ZFC condition. Afterwards, at the lowest temperature, a magnetic field of 100 G was applied and the magnetic moment of the sample was measured as the temperature increases. In the FC condition, the sample temperature is lowered to $T=2 \text{ K}$ from $T=300 \text{ K}$ in a field of 100 G. Once more, the magnetic moment of the sample is measured for increasing temperature.

2.2 Pressure measurements

In this part of the experiment, a SQUID piston cylinder cell (SPCC) (Appendix) was used as the equipment for pressure application. The maximum pressure for this cell is said to be $P_{\text{max}} \approx 1.4 \text{ GPa}$. At higher pressures parts of the cell may potentially deform [5]. Part of the sample from the LDPE can was transferred into the sample holder, a polytetrafluoroethylene (PTFE) can or Teflon can with a piece of superconducting lead (Pb) as the manometer. The phase transition of Pb from paramagnetic to a diamagnetic, allow us to calculate the pressure of the system using the linear relationship

$$\frac{\Delta T_c}{\Delta P} = 0.405 \text{ K/GPa}_a \quad (2.1)$$

where ΔT_c indicates the difference between the critical temperature of Pb at ambient pressure and the critical temperature at $P > \text{ambient}$. Since measurements were performed at low temperatures, using a low field (10 G) helped accentuate the sharpness of the phase transition plots seen on Figure 2.

Since three of the pressure measurements appeared to be the same regardless, a strategic procedure was taken in order to obtain precise pressure measurements. A curve was made (refer to Figure 2) with the purpose of simulating the “correct” path of the transition in order to get a more exact measure of the critical temperature, especially for the clustered measurements shown on Figure 2 (b).

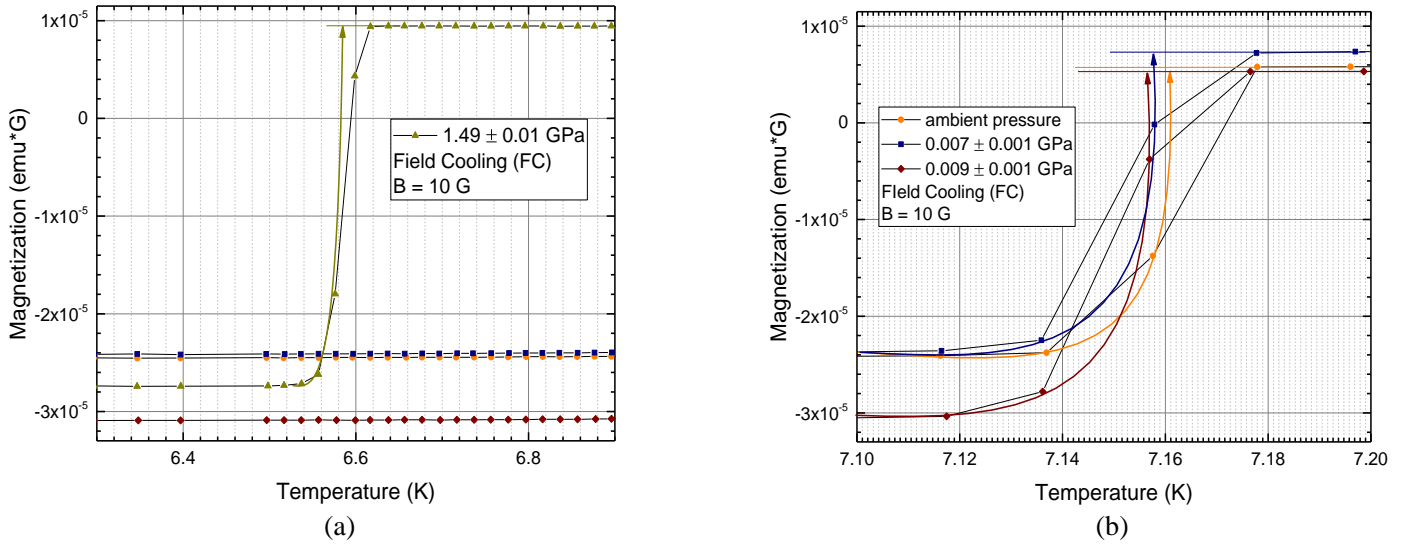


Figure 2. Expanded view for the lead superconducting transition at the different pressures in $B = 10 \text{ G}$. (a) Pb phase transition at the highest applied pressure for the SPCC. (b) Pb phase transition for ambient, slightly pressurized and the final released pressure. The drawn curves for (a) and (b) indicate the corresponding critical temperature tabulated on Table 1. The black lines are connecting the data points for easy eye tracking.

The same protocol of ZFC and FC were made with a few adjustments on the sequence run. This time, the sequence was set to make a run for two different fields, $B = 100 \text{ G}$ and $B = 1 \text{ kG}$. Furthermore, a measurement with $B = 10 \text{ G}$ was made in order to perform a more precise calculation of the pressure, as the phase transition from the normal state to the superconducting

state of Pb gives a sharper reading on this field. The reason for performing the measurement using a magnetic field of 1 kG was because the superconducting transition of the lead sits at a field of $B \leq 800$ G for a fixed critical temperature and pressure. Through these measurements, the effect of the lead superconducting transition on the sample reading was avoided in contrast to the measurements using a magnetic field of 100 G. These measurements were performed three times at different pressures, using all three magnetic fields. Lastly, a measurement was made by relaxing the pressure on the SPCC in order to detect if this process was reversible. The final measurement was made with the Pb alone inside the Teflon can in order to make future background subtraction from the pressure measurements.

2.3 Data analysis

Both Padé approximation (PA) and Cuire law (CL) were used in order to determine the antiferromagnetic and the paramagnetic components of the sample, respectively. The molar magnetic susceptibility for a Heisenberg antiferromagnetic spin chain using PA takes the form,

$$\chi_{mol}(J_{nn}, T) = \frac{N_A \mu_B^2 g^2 S(S+1)}{3K_B T} \times e^{\frac{\Delta J_{nn}}{K_B T}} \times \frac{1 + \sum_{i=1}^m A_i \left(\frac{\Delta J_{nn}}{K_B T}\right)^i}{1 + \sum_{j=1}^n B_j \left(\frac{\Delta J_{nn}}{K_B T}\right)^j} \quad (2.3.1)$$

where N_A is the Avogadro's number, K_B is the Boltzman constant, μ_B corresponds to Borh's magneton, g is the g -factor, Δ refers to the relative gap between the $S = 0$ and the excited spin states and J_{nn} is the known nearest-neighbor intrachain magnetic exchange. A_i and B_j are tabulated constants from the PA, in this case the ones corresponding to $S = 1$ [6]. The Curie law,

$$\chi = \frac{N_A \mu_B^2 g^2}{3K_B T} S(S + 1) \quad (2.3.2)$$

varies as C/T , where C is a constant that depends on the spin value. (2.3.2) is only valid when $B/K_B T$ is small enough [3]. The approximations for both PM and AFM components were performed on the high pressure and low pressure (ambient) measurements. The programing language MATLAB® was used in order to obtain the molar magnetic susceptibility using the PA for spin-1 Heisenberg chain together with the CL (refer to Appendix). Using the same programing language, the parameters J and g as well as a factor from the non-interacting paramagnetic $S = 1$ spins were adjusted in order to obtain the closest agreement possible by eye. Finally, the program OriginLab® was used as the software for plotting and figure editing.

Table 1. Rundown for all of the measurements chronologically described with specifications on mass, applied field, Pb critical temperatures, pressure and the parameters g-factor, J and PM factor used on the data analysis. The value for the parameters g, J and PM factor shown are the ones obtained without normalization. *Measurements were also performed at 10 G in order to obtain precise critical temperature values. **Measurements only performed with B = 100 G. NA = Not applicable.

Measurement number	and description	Sample mass (mg)	Field (B)	Pb T _c values (K)*	Pressure (GPa)	Parameters for analysis		
						g	J (K)	PM %
0	Plastic can with oil, mounted in straw	NA	100 G	NA	ambient	NA	NA	NA
1	Plastic can with oil and sample, mounted in straw	68.89 ±0.01	100 G	NA	ambient	1.8	5.4	8
2	Teflon can with oil, Pb and sample, mounted in straw	9.57 ±0.01	100 G	NA**	ambient	NA	NA	NA
3	Teflon can with oil, Pb, and sample, inside pressure cell	9.57 ±0.01	1 kG	6.49 ± 0.01	0.000 ±0.001	1.6	5.7	12
4	Teflon can with oil, Pb, and sample, inside pressure cell	9.57 ±0.01	1 kG	7.161 ± 0.001	0.007 ± 0.001	1.6	5.8	11
5	Teflon can with oil, Pb, and sample, inside pressure cell	9.57 ±0.01	1 kG	7.158 ± 0.001	1.49 ± 0.01	1.6	2.1	7
6	Teflon can with oil, Pb and sample inside the pressure cell	9.57 ±0.01	1 kG	7.157 ± 0.001	0.009 ± 0.001	1.6	5.6	11
7	Teflon can with Pb inside pressure cell	NA	1 kG	NA	NA	NA	NA	NA

3. Results and Discussion

3.1 Sample in $B = 100\text{ G}$ at ambient pressure

The magnetization as a function of temperature for the sample inside the LDPE can be shown on Figure 3 (a) as well as the background signal obtained from the can with the oil each with its corresponding error bars. The error bars, which appears to be the size of the data points, corresponds to $err = \sqrt{e_{raw}^2 + e_{bk}^2}$ where e_{raw} and e_{bk} are the raw data error and background error, respectively. The raw data from (b) indicated as orange dots, was obtained using point-by-point subtraction from the background signal from (a), and it is expressed as the susceptibility in GSI units. The UF sample data was normalized in order to match the data from J. L. Manson et al. [1] by 1.358 (to match the $T = 2\text{ K}$ data points). The mass of the sample, refer to Table 1. is used in order to obtain the susceptibility per mol. This data set resembles the fingerprint previously observed from J.L Manson et al [2]. No significant difference between ZFC and FC was observed (Appendix) .The curve observed at $5\text{ K} < T < 6\text{ K}$ is representative of the intrachain magnetic exchange along with a high Curie “tail” at $T < 4\text{ K}$.

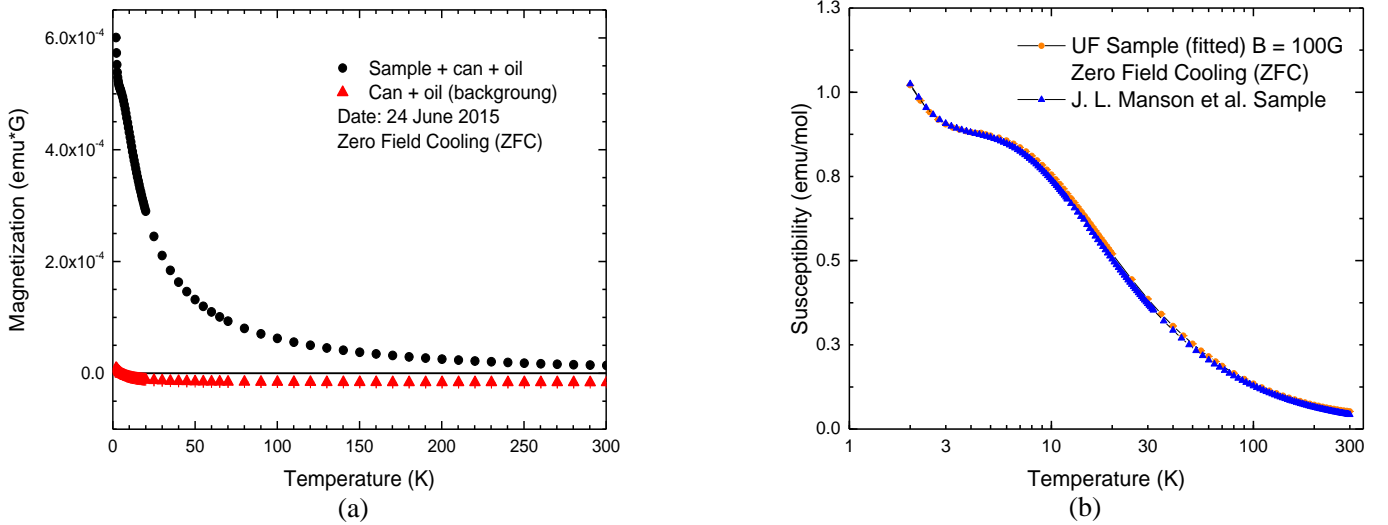


Figure 3. (a) ZFC magnetization data for $2\text{ K} \leq T \leq 300\text{ K}$ on $B = 100\text{ G}$ of the LDPE can with Daphne oil inside the plastic straw before and after inserting the sample. (b) ZFC susceptibility plot of the sample obtained after point-by-point subtraction from (a) and multiplied by 1.358 (to match the $T = 2\text{ K}$ data points), and the data from Figure 3 in Ref. 1 (converted to cgs units). The x-axis scale is logarithmic.

3.2 Sample inside the pressure cell

Results for the susceptibility as T decreases with $B = 1\text{ kG}$ for each pressure measurement are shown on Figure 4 (a). The intention was to linearly increase the pressure for each run, and in

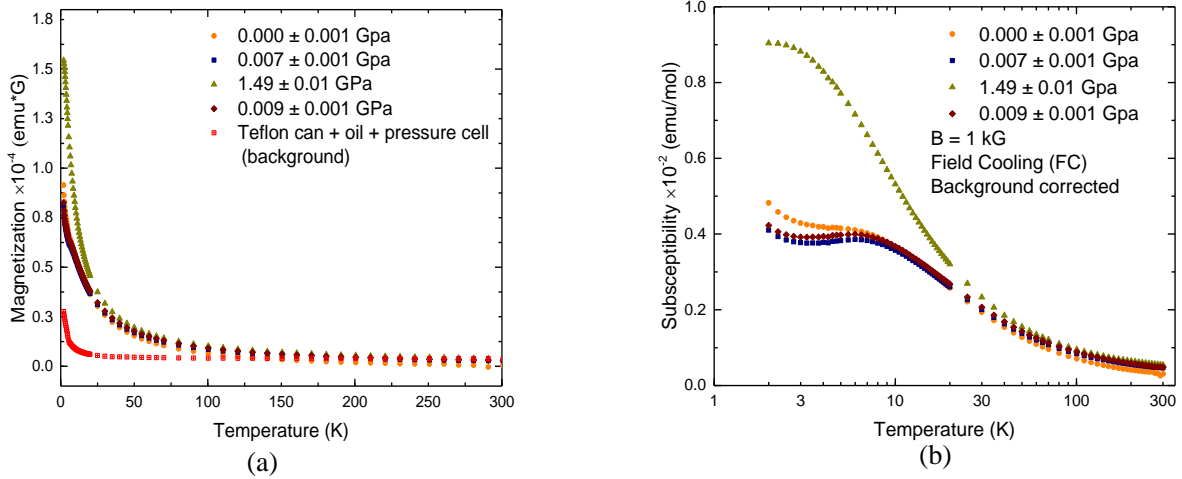


Figure 4. FC magnetization data for $2\text{ K} \leq T \leq 300\text{ K}$ on $B = 1\text{ kG}$ of the Teflon can with Daphne oil inside the pressure cell before and after inserting the sample. (b) FC susceptibility plot of the sample obtained after point-by-point subtraction from (a) and vertically adjusted to match the $T = 300\text{ K}$ data points from the ambient measurement on Figure 2 (b). The x-axis scale is logarithmic. Refer to Table 1 and section 2.2.1 for details about the pressure calculations acquisition. Legends chronologically list the pressure history of the sample.

the end, slightly release it to detect a possible reversible process. As for the result, shown on Figure 4 (b), the critical temperatures for the superconducting transition of Pb at $B = 10\text{ G}$ for the first two pressures (ambient and slightly pressurized) are, to a high degree, similar. Akin for the released pressure measurement. . It can be observed also on (a) as the only dramatic change is seen on the measurement for $P \approx 1.4\text{ GPa}$. The curve representing the exchange interaction seems to greatly shift from $T \approx 5\text{ K}$ to $T \approx 3\text{ K}$, as well as increasing the magnetization as T decreases. The Curie “tail” on the ambient measurement seems to outstand more than for those with a slight pressure difference. The last measurement (released pressure) result from the plot suggests that the process is indeed reversible, giving that the sample “finger print” seems preserved.

3.3 Paramagnetic and Antiferromagnetic contributions

Figure 5 contains the susceptibility measurements for each pressure, along with their respective paramagnetic and antiferromagnetic components using the Curie law and the Padé approximation for $S = 1$ Heisenberg chain. The modified parameters in order to obtain a suitable simulation of the data are the g -factor, a paramagnetic contribution percentage (PM factor), and the intrachain exchange interaction J . As a result, the g -factor seems to fluctuate around values from 1.6 to 1.65, hence it can be said that no pressure dependency is shown on this parameter. The PM factor varies between 11-13 % for the similar pressure measurements, for the high pressure case (~ 1.4 GPa) this PM factor reduced to $\sim 7\%$. In this PM factor, there seems to be a decreasing behavior as the pressure increases. The exchange interaction value ranges along the values of 5.6 K-5.8 K for the similar pressure measurements. For high pressure, the J value decreased more than a half, to 2.10 K. It is clearly shown on Figure 5 (c) that the AFM contribution suppresses the PM contribution on the high pressure data, supporting the fact that the PM factor behaves inversely proportional to the pressure.

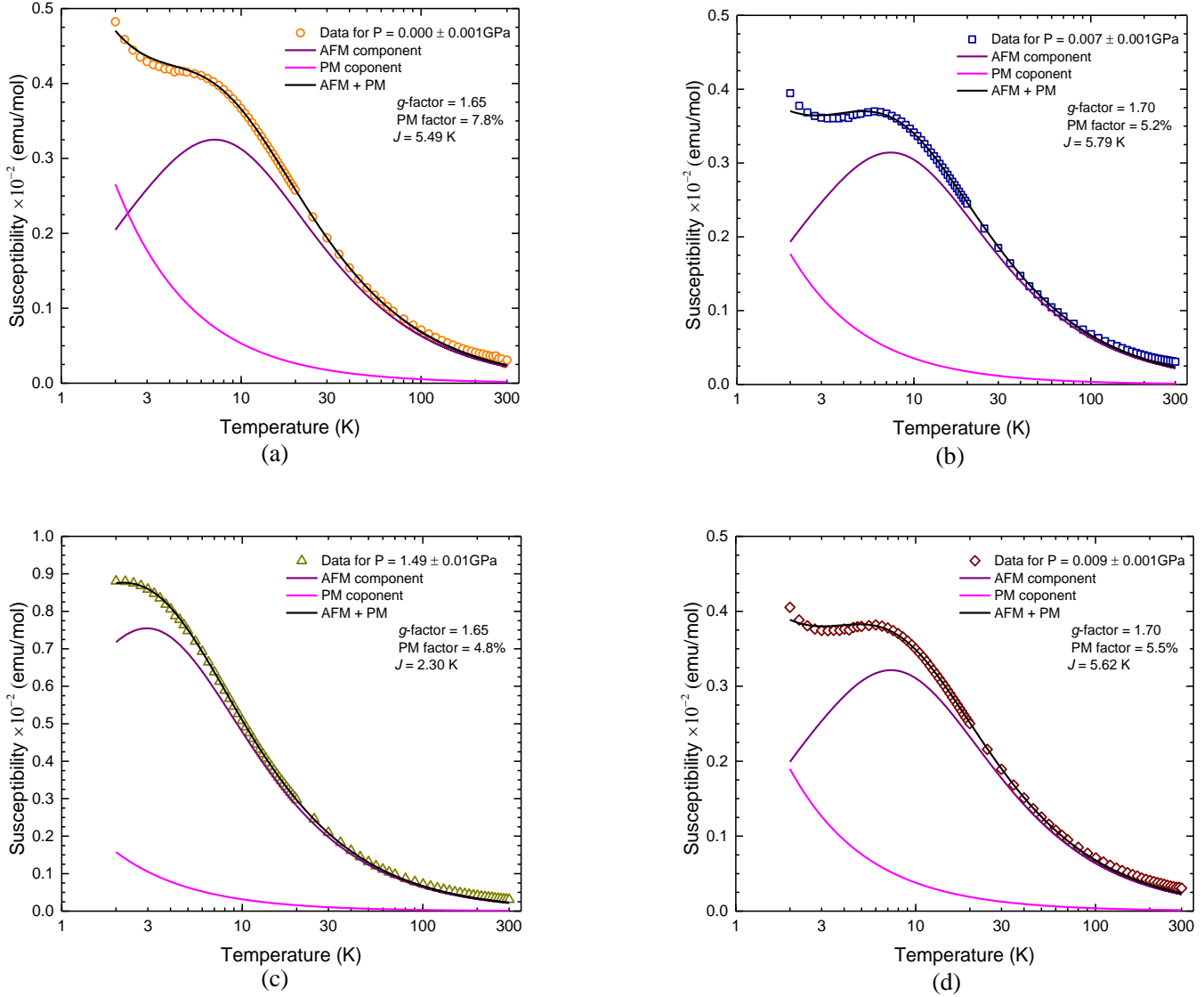


Figure 5. Background subtracted and corrected data (refer to Figure 4) for the Susceptibility as T decreases in $B = 1$ kG at different pressures with each respective PM and AFM components. The data points were normalized at $T = 300$ K. The parameters: g -factor, J and P.M. that were modified in order to obtain the simulations results listed in Table 1. The simulation is denoted as the black line.

4. Summary

The conjecture for the normalization factor needed on the comparison between our first measurement and the data of Manson et al. [2] lies upon whether or not the solvent used for the sample was causing the total mass of our sample to be over-estimated. With the application of pressure, a clear increase of the magnetization, as same for the susceptibility, is observed at high pressure. From the simulations, the high pressure measurement exhibits a strong antiferromagnetic contribution while suppressing the paramagnetic component, eliminating the “Curie-tail” effect at low temperatures when compared to the ambient and near ambient measurements. The results supports a pressure dependence behavior on the magnetic exchange interaction and the paramagnetic factor of the polymeric chain material. Furthermore, more pressure measurements are needed in order to confirm a linear dependency for one or both of these parameters. Electron paramagnetic resonance (EPR) can also be used in future studies in order to determine the value of the single-ion anisotropy under pressure and in order to determine the “new” D/J value.

Acknowledgements

Special thanks to the University of Florida REU program and director Dr. Hershfield for coordinating this remarkable summer experience. In addition, special recognition to the supportive Merisel’s team composed by Marcus K. Peprah, Pedro A. Quientero, Brandon Blasiola and advisor Dr. Mark Meisel. This material is based on work supported by the National Science Foundation (NSF) under grants DMR-1461019 (UF Physics REU Program support for JMP), DMR-1202033 (MWM), DMR-1306158 (JLM), and DMR-1157490 (NHMFL), and by the State of Florida.

5. Appendix

5.1 SQUID and extension tools

All the data collected was with the use of the Quantum Design SQUID magnetometer, Figure 6 (a). The model used in this experiment was the MPMS-XL7 equipped with a 7 T superconducting magnet. The sample space can operate below 4.2 K due to the addition of a low temperature continuous impedance tube [5]. The magnetometer works detecting the magnetic moment of a sample by moving it through a set of superconducting pick-up coils as shown on Figure 6 (b). The detection arrangement of these set of coils starts with an upper single-turn (clockwise) coil followed by a middle double-turn (counterclockwise) coil and finishing by a lower single-turn (clockwise) coil. A current is induced in the coils as the sample is moved through them and it is proportional to the magnetic moment of the sample.

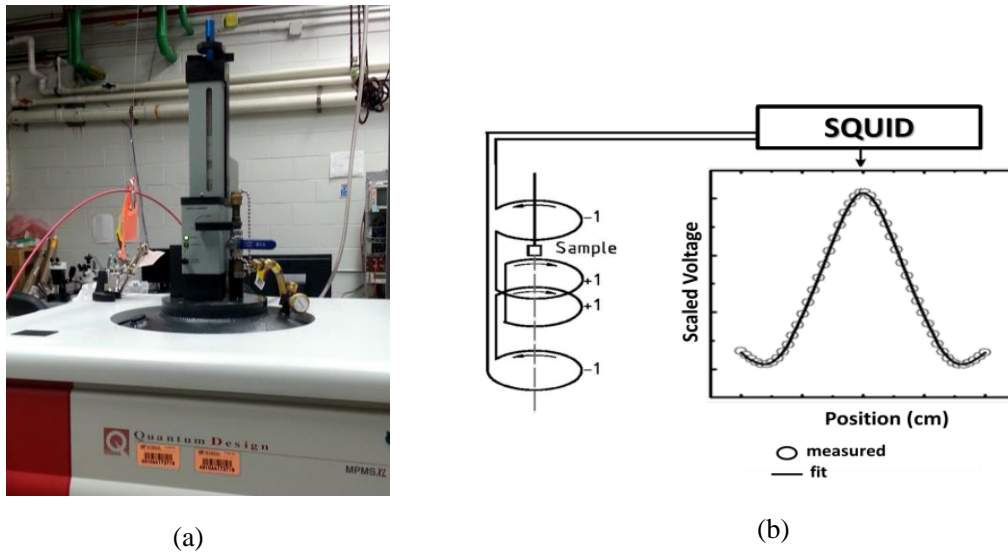


Figure 6. (a) Picture of the MPMS-XL7 SQUID magnetometer. (b) Illustrative diagram for the detection coils and induced voltage as function of the sample position. The coils are placed at the center of the superconducting magnet as the sample is moved through the coils in an applied field. The induced current is proportional to the change in magnetic flux which corresponds to a change in the SQUID output voltage. These changes are then converted to the magnetic moment of the sample. Diagram from: M.K. Peprah [5].

A plastic straw was attached to the (MPMS) transport rod as shown on Figure 7 (a) for the first measurement. The plastic straw holds the sample holder (low density polyethylene (LDPE) can) containing the sample along with the oil as shown on (a.1).

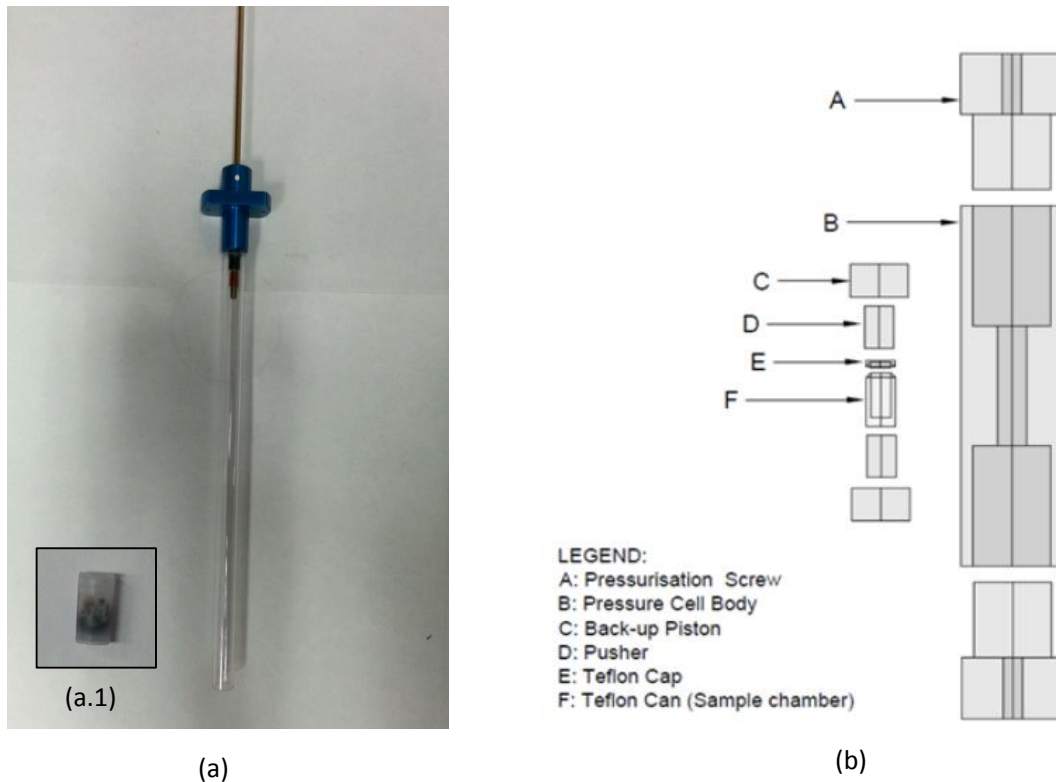


Figure 7. (a) Picture of the magnetic property measurement system (MPMS) transport rod. The length of the plastic tube that holds the straw with the sample can is 16 cm. Attached is a picture of the plastic can with the sample and the oil used for the first measurement. The scale of the picture is set by diameter of can, which is 7 mm. (b) Diagram of the SQUID piston cylinder cell (SPCC) used for pressure measurements. This pressure cell is replaced for the plastic straw on the transport rod. The legend indicates each part of the cell and the Teflon sample holder. Diagram acquired from M.K. Pehrah [5].

A pressure cell made from beryllium copper (BeCu) cell was used as the tool for the pressure measurements. A diagram of this cell is shown on Figure 7 (b). The sample holder with the cap are both made from Teflon. For pressure application, screws are turned alternatively to increase the pressure on the sample [5].

5.2 Data Analysis MATLAB® Program

The program plots the data given by the susceptibility vector obtained from Figure 5, the Curie Law (paramagnetic contribution), the Padé approximation (antiferromagnetic contribution) and the sum of these last two. The parameters g , J , and PM factor were manually modified in order to better simulate the data plot to the sum of the PM and AFM contributions. This example of the code uses the values of the parameters that yield the results shown on Figure 5 (c).

```
clear all
hold on
temp = [];% Temperature vector
subs = [];% Susceptibility data
kb = 1.38045*10^(-23);
N = 6.023*10^(23);
uB = 9.274*10^(-24);
d_gap = -0.41191;
s = 1;
Jfhf = 2.3; % Adjusted Parameter
g = 1.65; % Adjusted Parameter
PMf = 4.8; % Adjusted Parameter
T0 = 2;
deltaT = 0.1;
Tf = 300;
A = [0.67855;1.2698;0.65478;0.14123;0.087773;-9.1750*10^(-5)];
B = [1.6000;2.6533;2.5159;1.6783;0.41951;0.041205];
T = T0:deltaT:Tf;
for j = 1:length(T)
    a = 1;
    b = 1;
    for i = 1:length(A)
        a = a + A(i)*(Jfhf/(T(j)))^i;
        b = b + B(i)*(Jfhf/(T(j)))^i;
    end
    x1(j) = 0.125105*(g^2*s*(s+1)/(T(j)))*exp((d_gap*Jfhf/T(j))*(a/b)); % P.A.

    x2(j) = 0.125105*PMf*(g^2*s*(s+1)/T(j)); % Curie Law
end
X = x1 + x2;
figure1 = figure(1); clf; hold on; box on;
plot(temp,subs,'oK')
plot(T,x1,'b')
plot(T,x2,'m')
plot(T,X,'-k')
set(gca,'xscale','log');
title('T-dependent magnetic properties for NiHF2 chain S=1')
legend('Data','Pade aprox.','Curie law.','P.A. + C.L.')
xlabel('T')
ylabel('suscpetibility X (cm^3/mol)')
```

References:

- [1] J.S Xia, A. Ozarowski, P.M. Spurgeon, A.G. Baldwin, J.L. Manson, M.W. Meisel, "Unusual Magnetic Response for an $S=1$ Antiferromagnetic Linear-Chain Material" (2014) arXiv: 1409.5971, doi: <http://arxiv.org/abs/1409.5971>.
- [2] J.L. Manson, A.G. Baldwin, B.L. Scott, J. Bendix, R.E. Del Sesto, P.A. Goddard, Y. Kohama, H.E. Tran, S. Ghannadzadeh, J. Singleton, T. Lancanster, J.S. Möller, S.J. Blundell, F.L. Pratt, V.S. Zapf, J. Kang, C. Lee, M. Whangbo and C. Baines, "[Ni(HF₂)(3-Clpy)₄]BF₄ (py = pyridine): Evidence for Spin Exchange Along Strongly Distorted F•••H•••F– Bridges in a One-Dimensional Polymeric Chain", *Inorganic Chemistry* 51 (2012) 7520-7528, doi: 10.1021/ic300111k.
- [3] O. Kahn, *Molecular Magnetism*. New York, NY: VCH, 1993.
- [4] Y. Nakamura, A. Takimoto and M. Matsui, "Rheology and Nonhydrostatic Pressure Evaluation of Solidified Oils including Daphne Oils by Observing Microsphere Deformation", *Journal of Physics: Conference Series* 215 (2010) 012176, doi:10.1088/17426596/215/1/012176.
- [5] M.K. Peprah, "Influence of Pressure and Light on the Magnetic Properties of Prussian Blue Analogues and Hofmann-like Frameworks", PhD Thesis (2015) University of Florida, Gainesville.
- [6] J.M. Law, H. Benner and R.K. Kremer, "Padé Approximations for the Magnetic Susceptibilities of Heisenberg Antiferromagnetic Spin Chains for Various Spin Values", *Journal of Physics: Condensed Matter* 25 (2013) 065601, doi:10.1088/0953-8984/25/6/065601.
- [7] M. Orendáč, S. Zvyagin, A. Orendáčová, M. Sieling, B. Lüthi, A. Feher, and M. W. Meisel, "Single-ion bound states in $S=1$ Heisenberg antiferromagnetic chains with planar anisotropy and subcritical exchange coupling", *Physical Review B* 60 (1999) 4170-4175, doi:10.1103/PhysRevB.60.4170.